Table V. Smoothed Values of Stearic Acid in Various Solvents

(Temperature, °C. Solubility, g/100 g solvent)

CH_2Cl_2	
25	3.58
30	8.85
35	18.3

$CCl_2FCClF_2 + (CH_3)_2CHOH$	
20	1.50
25	2.38
30	3.81
35	6.18

$CCl_2FCClF_2 + CH_2Cl_2$	
10	0.31
15	0.82
20	1.97
25	4.33
30	8.84
35	17.0

CCl_2FCCl_2F	
30	2.61
35	5.33
40	11.0
45	22.7

CCl_3CF_3	
30	0.69
35	1.58
40	3.85

$CCl_2FCClF_2 + (CH_3)_2CO$	
20	0.86
25	1.52
30	2.74
35	5.09
40	9.72

CCl_4	
25	5.47
30	10.6
35	18.8
40	30.9

CH_3CCl_3	
25	4.79
30	8.67
35	16.3

$CCl_2FCClF_2 + CHCl_3$	
20	0.22
25	0.56
30	1.35
35	3.16

$CCl_2FCClF_2 + CH_3CH_2OH$	
25	3.22
30	5.37
35	8.99
40	15.1

CH_3CH_2OH (760 ppm H_2O)	
15	0.79
20	1.27
25	2.23
30	4.35
35	9.86
40	27.3

CCl_2FCClF_2	
25	0.28
30	0.68
35	1.67
40	4.23
45	11.0

CF_2BrCF_2Br	
25	0.30
30	0.79
35	1.92

Table VI. Effect of Water Concentration on Stearic Acid Solubility in Ethanol

	Solubility, g/100 g solvent		
	This work,	Ralston and Hoerr (*6*)	
Temp, °C	760 ppm H_2O	50,000 ppm	6000 ppm
20	1.27	1.13	2.24
30	4.35	3.42	5.43
40	27.3	17.1	22.7

LITERATURE CITED

(1) Brandreth, D. A., Molstad, M. C., *J. Chem. Eng. Data*, **7**, 449 (1962).
(2) Brown, J. B., Foreman, H. D., *Oil Soap*, **21**, 183 (1944).
(3) Brown, J. B., Kolb, D. K., *J. Amer. Oil Chem. Soc.*, **32**, 357 (1955).
(4) Francis, F., Collings, F. J. E., Piper, S. H., *Proc. Roy. Soc.*, Ser. A. **158**, 691 (1937).
(5) Preckshot, G. W., Nouri, F. J., *J. Amer. Oil Chem. Soc.*, **34**, 151 (1957).
(6) Ralston, A. W., Hoerr, C. W., *J. Org. Chem.*, **7**, 546 (1942).
(7) Ralston, A. W., Hoerr, C. W., *ibid.*, **9**, 329 (1944).
(8) Ralston, A. W., Hoerr, C. W., Sedgwick, R. S., *ibid.*, **11**, 603 (1946).
(9) Scarborough, J. B., "Numerical Mathematical Analysis," 4th ed., p 478, Johns-Hopkins Press, Baltimore, Md., 1958.
(10) Singleton, W. S., Ward, T. L., Dollear, F. G., *J. Amer. Oil Chem. Soc.*, **27**, 143 (1950).
(11) Taylor, H. S., "A Treatise on Physical Chemistry," Vol. I, 2nd ed., p 535, Van Nostrand, New York, N. Y., 1931.
(12) Timmermans, J., "Physico-chemical Constants of Pure Organic Compounds," p 402, Elsevier, New York, N. Y., 1950.
(13) von Sydow, E., *Acta Chem. Scand.*, **9**, 1119 (1955).
(14) Zellhoffer, G. F., Copley, M. J., Marvel, C. S., *J. Amer. Chem. Soc.*, **61**, 3350 (1939).

RECEIVED for review May 12, 1970. Accepted February 19, 1971. Contribution No. 463, Experimental Station, Research and Development Division, Organic Chemicals Department, E. I. du Pont de Nemours and Co., Inc., Wilmington, Del. 19898.

Pore-Size Distributions of Copper Oxide–Alumina Catalysts

CHIEH CHU, MUCHLAS HAMIDY, and KEN NOBE[1]

School of Engineering and Applied Science, University of California, Los Angeles, Calif. 90024

Six copper oxide–alumina catalysts were prepared using cupric chloride, bromide, nitrate, or sulfate in conjunction with sodium or potassium hydroxide, with wet or dry alumina as the carrier. The pore-size distributions were determined by the Cranston-Inkley method, based on adsorption isotherms. The resulting distributions, unimodal or multimodal, were adequately represented by simple or complex Weibull distributions. The surface areas based on the Cranston-Inkley method were compared with the BET areas.

In recent years copper oxide–alumina catalysts assumed increased importance because of their effectiveness in the removal of carbon monoxide, hydrocarbons, and nitrogen oxides which exist in the automobile exhaust emissions. (See, for example, refs. *1*, *3*, and *11*.) Copper oxide catalysts prepared in different ways showed different catalytic activities. In an attempt partially to explain the variation in catalyst performance, the pore-size distributions of six copper oxide–alumina catalysts with approximately the same chemical composition but prepared with different raw materials were determined. It is expected that differences in the pore structure of the catalysts may affect catalyst effectiveness, reaction selectivity, surface stability, susceptibility to poisoning, as well as heat transfer characteristics (*8*).

The pore-size distributions of a large family of silica gels were found by Wheeler (*10*) to follow approximately a normal distribution. Debaun et al. (*5*) reported that

[1] To whom correspondence should be addressed.

many cracking, reforming, and hydrodesulfurization catalysts had a log normal distribution. This work shows that copper oxide–alumina catalysts can be adequately represented by simple or complex Weibull distributions (*9*).

EXPERIMENTAL

The catalysts prepared in this work were in pellet form, 3 mm in diameter and 2.5 mm in length, and contained approximately 50% CuO and 50% alumina by weight. They were prepared as follows:

Catalyst No. 1. Cupric chloride ($CuCl_2 \cdot 2H_2O$, 99.6% purity, Baker and Adamson quality product) was dissolved in distilled water. Wet alumina (28% Al_2O_3, filtrol alumina grade 90, in gel form), in an amount which would produce a catalyst with the 50-50 composition mentioned above, was slowly added to the solution, with continued stirring. The mixture was then heated to approximately 90° C. After 15 min, sodium hydroxide solution, with 25% excess, was added very slowly to the mixture. As the mixture changed from an acidic to a basic condition, its color changed from green to brown and finally to black. The mixture was filtered and washed with distilled water, until a neutral filtrate was obtained. The precipitate was now $Cu(OH)_2$ on alumina. It was put in the catalyst molds and heated in the oven for 36 hr at 200° C to convert $Cu(OH)_2$ to CuO.

Catalyst No. 2. The procedure was the same as above except that cupric bromide ($CuBr_2$, 99.6% quality, Baker and Adamson quality product) was used in the solution and cupric hydroxide was precipitated by the addition of a stoichiometric quantity of sodium hydroxide solution.

Catalyst No. 3. Cupric nitrate [$Cu(NO_3)_2 \cdot 3H_2O$, 99.5% quality, Baker and Adamson quality product] was dissolved in distilled water and added to wet alumina. The mixture was then stirred and sodium hydroxide was added crystal by crystal until the mixture became basic. Filtration and washing followed.

Catalyst No. 4. The procedure was the same as that for Catalyst No. 1 except that cupric sulfate ($CuSO_4 \cdot 5H_2O$, 99.6% purity, Baker and Adamson quality product) was used and 77% excess sodium hydroxide solution was added.

Catalyst No. 5. The procedure was again the same as that for Catalyst No. 1 except that cupric nitrate was used and a stoichiometric quantity of potassium hydroxide solution was added.

Catalyst No. 6. A cupric nitrate solution was mixed with a correct amount of dry alumina. A stoichiometric quantity of sodium hydroxide solution was then added to the mixture with continual stirring. Filtration and washing followed.

A summary of the raw materials used in different catalysts is shown in Table I.

The adsorption-desorption isotherms were determined by using nitrogen as the adsorption gas with the catalyst samples maintained at −195.8° C. During adsorption, the absolute pressure was raised in stages from as low as 5 mm Hg to as high as 767 mm Hg. During desorption the pressure was brought down to as low as 340 mm Hg, also in stages. The complete adsorption and desorption data were reported elsewhere (*7*).

RESULTS AND DISCUSSION

Pore-size distributions were calculated by the Cranston-Inkley method (*4*), based on adsorption isotherms. The choice of adsorption isotherms was made because they usually led to more reasonable pore-size distributions (*8*). The pore-volume distributions are shown in Table II. Figure 1 shows the unnormalized differential pore-volume distribution ($\Delta V/\Delta D$ vs. D) for Catalysts Nos. 1–6. The cumulative pore-volume distributions after normalization for Catalysts Nos. 1–3 are shown in Figure 2 and those for Catalysts Nos. 4–6 in Figure 3.

Table I. Raw Materials Used in Catalyst Preparation

Catalyst no.	Copper salt	Alkali	Carrier
1	$CuCl_2 \cdot 2H_2O$	NaOH solution	Wet alumina
2	$CuBr_2$	NaOH solution	Wet alumina
3	$Cu(NO_3)_2 \cdot 3H_2O$	NaOH crystals	Wet alumina
4	$CuSO_4 \cdot 5H_2O$	NaOH solution	Wet alumina
5	$Cu(NO_3)_2 \cdot 3H_2O$	KOH solution	Wet alumina
6	$Cu(NO_3)_2 \cdot 3H_2O$	NaOH solution	Dry alumina

Table II. Pore Volume Distributions

Range of pore diameters, Å	Pore volume, V, ml/g × 10³					
	No. 1	No. 2	No. 3	No. 4	No. 5	No. 6
290–300	0.8	1.2	0.6	3.1	0.4	2.0
280–290	1.6	0.4	0.8	0.8	0.8	1.7
270–280	1.2	0.6	0.4	3.1	0.8	2.3
260–270	1.3	1.3	0.8	2.3	1.2	3.5
250–260	5.3	1.2	1.0	2.0	2.0	1.7
240–250	2.0	0.8	0.6	1.8	0.8	2.1
230–240	2.4	1.6	0.8	1.8	2.2	2.4
220–230	2.2	1.2	0.8	2.8	1.6	3.4
210–220	3.4	2.2	0.8	2.8	3.0	3.0
200–210	2.8	0.8	0.8	2.8	3.2	4.4
190–200	3.2	1.4	0.8	3.2	1.2	3.2
180–190	3.0	1.2	1.4	3.2	2.7	3.6
170–180	1.8	0.8	1.2	3.0	1.6	3.2
160–170	3.0	1.0	1.2	3.3	3.1	3.0
150–160	4.2	0.8	1.0	3.7	3.1	6.1
140–150	2.9	1.0	0.8	4.6	4.5	4.4
130–140	3.8	1.7	1.7	4.0	3.4	5.7
120–130	3.8	0.8	5.7	4.1	3.6	4.6
110–120	6.6	1.7	1.5	3.9	3.9	4.6
100–110	4.7	2.2	4.2	7.2	5.6	6.1
90–100	4.2	1.7	4.2	5.8	5.3	4.4
80–90	4.8	2.8	4.7	6.3	6.4	4.1
70–80	6.3	2.7	5.5	4.9	5.0	1.6
60–70	4.5	2.7	9.3	5.3	6.6	6.8
50–60	6.1	5.9	9.5	5.0	7.7	3.5
45–50	2.2	2.4	6.1	2.2	5.1	1.0
40–45	1.3	3.0	6.0	0.3	7.0	0.7
35–40	1.8	1.9	7.8	0.3	6.6	1.9
30–35	0.5	3.6	8.1	0.3	5.2	2.6
25–30	0.3	...	12.2	1.3	6.7	6.8
20–25	6.4	...	2.9	8.0	12.1	14.6
18–20	1.3	...	...	6.1	7.3	9.5
16–18	6.2	...	...	4.5	15.3	11.0
14–16	15.2	...	...	1.0	7.0	11.8
Total	121.3	50.6	103.2	114.6	151.0	151.3

A unimodal pore-size distribution, typified by that of Catalyst No. 3, was fitted by a Weibull distribution. This distribution, just as all the other distributions that are applied to real populations from natural fields, does not have any theoretical basis. However, it has been applied to many widely different populations, such as the size distribution of fly ash and the fatigue life of an St-37 steel, with quite satisfactory results (*9*). The Weibull distribution is defined as follows:

Cumulative volume above D:

$$1 - F - \exp\left[-(D-\alpha)^{\beta}/\gamma\right] \qquad (1)$$

where D = pore diameter, Å, F = cumulative volume below D, and α, β, and γ are parameters. The corresponding volume density function is:

$$f = \frac{\beta(D-\alpha)^{\beta-1}}{\gamma} \exp\left[-\frac{(D-\alpha)^{\beta}}{\gamma}\right] \qquad (2)$$

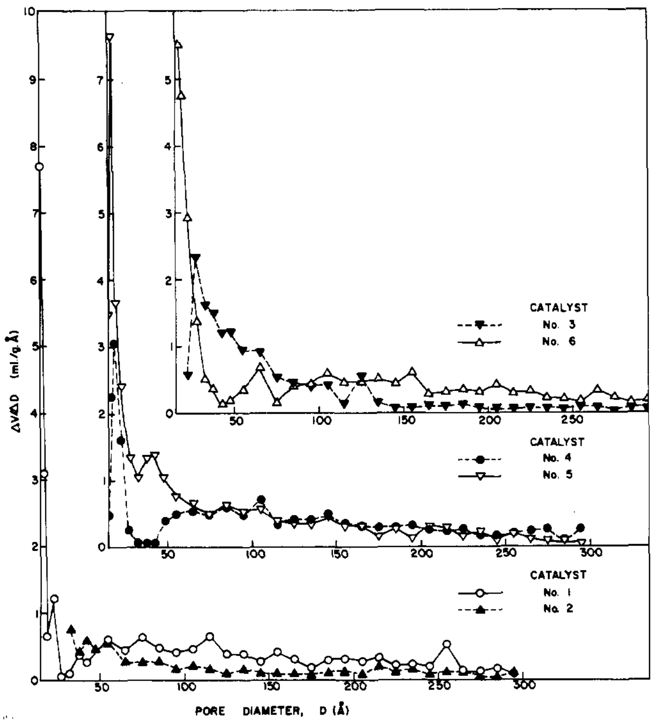

Figure 1. Unnormalized differential pore volume distributions for Catalysts Nos. 1–6

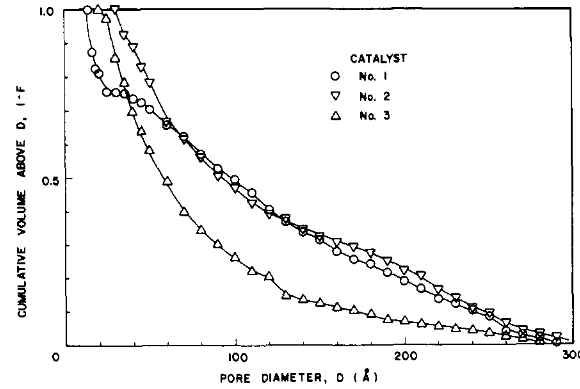

Figure 2. Cumulative pore volume distributions for Catalysts Nos. 1–3

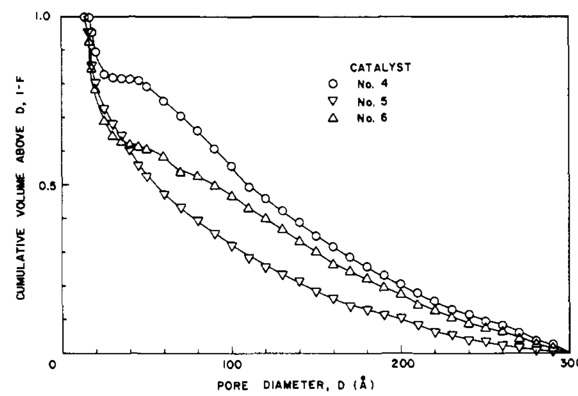

Figure 3. Cumulative pore volume distributions for Catalysts Nos. 4–6

In the determination of the parameters α, β, and γ, a series of α's was first chosen. For each α, the values of β and γ were calculated by least-squares treatment of the equation

$$\log\left[\log\left(\frac{1}{1-F}\right)\right] = \beta \log (D - \alpha) - \log \gamma \quad (3)$$

Then that α, with its associated β and γ, was chosen which gave the least sum of squares, namely,

$$\sum_j \left\{\log\left[\log\left(\frac{1}{1-F}\right)_j\right] - \beta \log (D_j - \alpha) + \log \gamma\right\}^2 \quad (4)$$

where j is the running index of pore diameters.

For comparison, the log normal distribution was also calculated which is defined as follows (*6*):

Cumulative volume above D:

$$1 - F = \frac{1}{(2\pi)^{1/2}} \int_{\frac{\log D - \mu}{\sigma}}^{\infty} \exp\left(-\frac{t^2}{2}\right) dt = \tfrac{1}{2} \operatorname{erfc}\left(\frac{\log D - \mu}{(2)^{1/2}\sigma}\right) \quad (5)$$

where erfc = complementary error function and μ and σ are parameters. The corresponding volume density function is:

$$f = \frac{1}{(2\pi)^{1/2}\sigma} \frac{1}{D} \exp\left[-\frac{(\log D - \mu)^2}{2\sigma^2}\right] \quad (6)$$

The parameters μ and σ were calculated by use of the following equations for the expected value and variance, respectively:

$$E(D) = \exp (\mu + \tfrac{1}{2}\sigma^2) \quad (7)$$

$$\operatorname{Var} (D) = \exp (2\mu + \sigma^2) [\exp (\sigma^2) - 1] \quad (8)$$

The experimental values of $(1 - F)$ and f for Catalyst No. 3 are shown in Figure 4, together with the calculated Weibull and log normal distributions that best fitted the data. It is evident that the simple Weibull distribution represents the experimental data adequately.

The pore-size distributions of some other catalysts could not be represented by a simple Weibull distribution and therefore a complex Weibull distribution had to be used. This was done by separating the experimental distribution into two or more sections; each section was fitted with a Weibull distribution. The choice of the number of sections was governed by the principle of parsimonious parametrization. In other words, the minimum number of sections was chosen which would adequately represent the experimental data. In this way, the cumulative volume distribution and the volume density function, respectively, are as follows:

$$1 - F = \sum_i \left\{(1 - F)_{ai} + [(1 - F)_{bi} - (1 - F)_{ai}] \times \exp\left[-\frac{(D - \alpha_i)^{\beta_i}}{\gamma_i}\right]\right\}[u(D - D_{bi}) - (D - D_{ai})] \quad (9)$$

$$f = [(1 - F)_{bi} - (1 - F)_{ai}] \frac{\beta_i (D - \alpha_i)^{\beta_i - 1}}{\gamma_i} \exp\left[-\frac{(D - \alpha_i)^{\beta_i}}{\gamma_i}\right] \quad (10)$$

In the above, i is the running index of sections, ai refers to the upper limit of pore sizes in section i, bi refers to the lower limit, and $u(D - D_{bi})$ is the unit step function which is equal to 1 for $D > D_{bi}$ but vanishes for $D < D_{bi}$. Similar sectionalizing was also done on the log normal distribution. The cumulative volume distribution and the volume-density function follow:

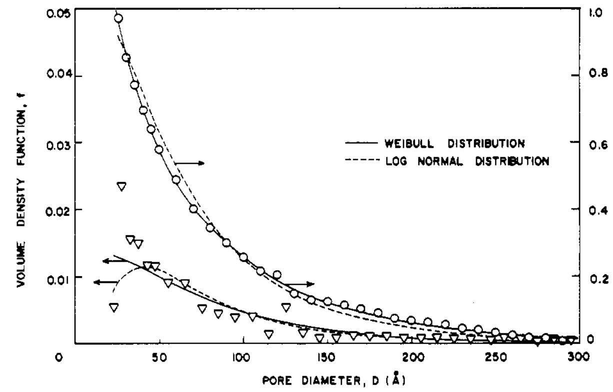

Figure 4. Comparison of experimental and calculated distributions for Catalyst No. 3

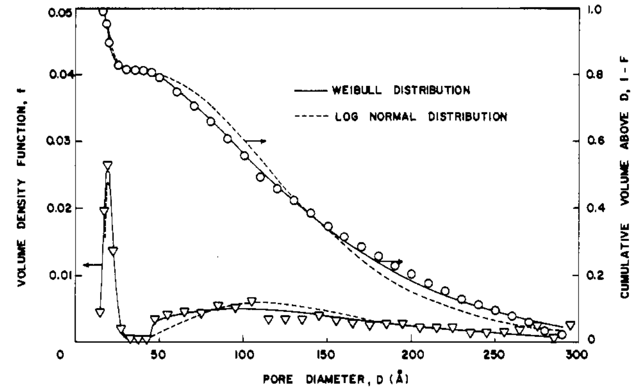

Figure 5. Comparison of experimental and calculated distributions for Catalyst No. 4

Table III. Information for Sectionalizing and Parameters for Weibull and Log Normal Distributions

	1	2	3	4	5	6
	Total no. of sections					
Catalyst no.	3	3	1	3	3	2
Section 1						
D_{a1}	300	300	300	300	300	300
D_{b1}	260	170	20	45	110	30
$(1 - F)_{a1}$	0.000	0.000	0.000	0.000	0.000	0.000
$(1 - F)_{b1}$	0.040	0.291	1.000	0.810	0.284	0.645
α_1	172.1	162.4	20.0	42.5	87.5	5.5
β_1	9.53	1.90	1.06	1.37	1.92	2.04
γ_1	0.307×10^{20}	0.399×10^{4}	82.3	0.702×10^{3}	0.738×10^{4}	0.329×10^{5}
μ_1	5.63	5.43	4.16	4.90	5.16	4.91
σ_1	0.038	0.149	0.676	0.451	0.266	0.448
Section 2						
D_{a2}	260	170		45	110	30
D_{b2}	30	60		30	20	14
$(1 - F)_{a2}$	0.040	0.291		0.810	0.284	0.645
$(1 - F)_{b2}$	0.756	0.668		0.818	0.805	1.000
α_2	30.0	52.8		30.0	11.9	13.3
β_2	1.52	1.56		1.44	1.39	1.45
γ_2	0.144×10^{4}	0.532×10^{3}		25.0	0.213×10^{3}	16.9
μ_2	4.80	4.59		3.62	3.88	2.96
σ_2	0.457	0.285		0.109	0.461	0.202
Section 3						
D_{a3}	30	60		30	20	
D_{b3}	14	30		14	14	
$(1 - F)_{a3}$	0.756	0.668		0.818	0.805	
$(1 - F)_{b3}$	1.000	1.000		1.000	1.000	
α_3	−27.4	−4.6		14.0	13.9	
β_3	9.42	4.66		2.38	2.46	
γ_3	0.347×10^{16}	0.115×10^{9}		96.6	23.0	
μ_3	2.84	3.79		3.00	2.83	
σ_3	0.179	0.194		0.149	0.082	

$$1 - F = \tfrac{1}{2} \sum_i \left\{ (1 - F)_{ai} + \left[(1 - F)_{bi} - (1 - F)_{ai} \right] \operatorname{erfc}\left(\frac{\log D - \mu_i}{(2)^{1/2} \sigma_i} \right) \right\} \left[u(D - D_{bi}) - u(D - D_{ai}) \right] \quad (11)$$

$$f = \frac{1}{(2\pi)^{1/2}} \left[\frac{1}{D} \left((1 - F)_{bi} - (1 - F)_{ai} \right) \right] \frac{1}{\sigma_i} \exp\left[- \frac{(\log D - \mu_i)^2}{2 \sigma_i^2} \right] \quad (12)$$

The information for sectionalizing and the parameters for Weibull and log normal distributions for the six catalysts are presented in Table III. (Catalyst No. 3 is also included with the number of sections which equals 1.) A typical distribution for which sectionalizing was necessary, that of Catalyst No. 4, is shown in Figure 5. Here, the experimental data are adequately represented by a complex Weibull distribution.

The surface areas and mean pore diameters are also of general interest. Table IV shows a comparison of surface areas calculated from the pore-size distributions by the Cranston-Inkley method (designated as the CI method) and the areas determined by the BET method (2). Except for Catalyst No. 6, the surface areas by the CI method are smaller than the BET areas. The same table also shows mean pore diameters based on pore volume, surface area, and number of pores. Because of the differences in pore-size distribution, the catalyst having the largest mean pore diameter based on volume does not necessarily have the largest mean diameter based on surface or number of pores.

Table IV. Surface Areas and Mean Pore Diameters

Catalyst no.	Surface areas, m^2/g		Mean pore diameters, D, Å, based on		
	BET	CI	Vol	Surface	No.
1	144	105.0	111.6	46.2	22.3
2	39	26.2	120.9	77.1	54.6
3	119	78.7	80.6	52.5	39.5
4	134	75.2	123.9	60.9	29.5
5	164	155.6	82.7	39.1	24.1
6	149	148.5	103.9	40.8	22.3

NOMENCLATURE

D = pore diameter, Å
E = expected value
F = cumulative volume below D
f = volume density function
t = dummy variable
u = unit step function
V = volume, ml/g
Var = variance

Greek Symbols

α = parameter in Weibull distribution
β = parameter in Weibull distribution
γ = parameter in Weibull distribution
μ = parameter in log normal distribution
σ = parameter in log normal distribution

Subscripts

ai = upper limit of pore sizes in section i
bi = lower limit of pore sizes in section i
i = running index of sections
j = running index of pore diameter

LITERATURE CITED

(1) Blumenthal, J. L., Nobe, K., *Ind. Eng. Chem. Proc. Des. Develop.*, **5**, 177 (1966).
(2) Brunauer, S., Emmett, P. M., Teller, E. J., *J. Amer. Chem. Soc.*, **60**, 309 (1938).
(3) Caretto, L. S., Nobe, K., *ibid.*, **5**, 217 (1966).
(4) Cranston, R. W., Inkley, F. A., *Adv. Catalysis*, **9**, 143–53 (1957).
(5) Debaun, R. M., Adler, S. F., Fink, R. D., *J. Chem. Eng. Data*, **7**, 94 (1962).
(6) Hald, A., "Statistical Theory with Engineering Applications," pp 160–74, Wiley, New York, N. Y., 1964.
(7) Hamidy, Muchlas, MS Thesis, University of California, Los Angeles, Calif., 1962.
(8) Innes, W. B., in "Experimental Methods in Catalytic Research," pp 44–99, R. B. Anderson, Ed., Academic Press, New York, N. Y., 1968.
(9) Weibull, W., *J. Appl. Mech.*, **18**, 293 (1951).
(10) Wheeler, A., *Catalysis*, Vol II, pp 111–18, P. M. Emmett, Ed., Reinhold, New York, N. Y., 1955.
(11) Wikstrom, L. L., Nobe, K., *Ind. Eng. Chem. Proc. Des. Develop.*, **4**, 191 (1965).

RECEIVED for review May 28, 1970. Accepted February 27, 1971. This work was supported by the UCLA air pollution research program. Some support was received from HEW Grant 1-R01-AP00913-01 National Air Pollution Control Administration.

Heat of Mixing of Water and Diethylene Glycol Dimethyl Ether

WILLIAM J. WALLACE[1] and THOMAS J. VELLENGA
Muskingum College, New Concord, Ohio 43762

Calorimetric heats of mixing have been obtained for the system water–diethylene glycol dimethyl ether at temperatures near 25° over the entire range of composition. The heat of mixing exhibits an exothermic maximum of 491 cal/mol of solution and an endothermic minimum of 57 cal/mol of solution, at mole fractions of diethylene glycol dimethyl ether equal to 0.115 and 0.86, respectively.

Diethylene glycol dimethyl ether is a useful solvent for a number of ionic reagents, notably sodium borohydride (*1, 5*). It is a colorless, mobile liquid, with a useful liquid range of over 200° C to its normal boiling point of 162° C, and it is miscible in all proportions with water. Some hydrated salts form anhydrous etherates when brought in contact with the ether (*5*). Considerable deviation from ideality is observed in density and viscosity data for water solutions of diethylene glycol dimethyl ether (*7*). We here report the heat of mixing of water with this ether over the full range of compositions at temperatures near 25° C. Temperature changes of up to 10° are observed, and the starting temperature was chosen so that the midpoint of the temperature change due to mixing was at 25° C.

EXPERIMENTAL

Materials. Diethylene glycol dimethyl ether (Ansul Chemical Co., Ether E-141, Diglyme) was distilled from sodium under a nitrogen atmosphere at 162–3° C (uncorr.) and gave a negative peroxide test (*2*). Water content was less than 0.01% based on Karl Fischer electrometric titrations. Water was freshly distilled for each determination. Densities, refractive indexes, molar refractions, and viscosities of water–diethylene glycol dimethyl ether have been reported previously (*7*).

Calorimeter. The calorimeter consisted of an ordinary one-pint Dewar flask fitted with a stirrer, thermometer, and one of three inner vessels as shown in Figure 1. Choice of the inner vessel used depended on the desired final concentration. The procedure followed consisted of weighing the liquid of larger amount into the Dewar flask, and the other liquid into the inner vessel. The apparatus was assembled and the contents were warmed sufficiently to result in a temperature change during mixing which would be equally above and below 25° C. The stirrer was actuated by a reciprocating takeoff on an ordinary stirring motor. Temperature readings were made at regular intervals during each determination.

The liquids were mixed by crushing the thin-walled inner vessel against the bottom of the Dewar, or, in the case of the stoppered inner vessel, by opening the stopper and forcing the liquid out with a surge of dry air. The inner

[1] To whom correspondence should be addressed.